energies

Article

Self-Cleaning Mortar Façades with Addition of Anatase and Rutile Titanium Dioxide for Cool Façades

Eduardo Linhares Qualharini [1,*], Carina Mariane Stolz [1], Matheus Martini [2], Eduardo Polesello [3] and Clara Rocha da Silva [4]

1 Escola Politécnica, Universidade Federal do Rio de Janeiro, Rio de Janeiro 21941-901, Brazil
2 Onex Engenharia, Novo Hamburgo 93546-010, Brazil
3 Instituto de Ciências Criativas e Tecnológicas, Universidade FEEVALE, Novo Hamburgo 93300-000, Brazil
4 Programa de Engenharia Ambiental, Universidade Federal do Rio de Janeiro, Rio de Janeiro 21941-901, Brazil
* Correspondence: qualharini@poli.ufrj.br; Tel.: +55-21-3938-7965

Abstract: The concern with the best energy performance of buildings is a current theme, and construction materials that bring improvements to the performance of buildings and their surroundings are in demand. Façades play a crucial role in regulating the temperature within buildings by permitting or obstructing the transfer of heat and also affect the ambient temperature. Light-colored façades help maintain environments with milder temperatures, but pollution, rain, and other degrading agents darken the colors of the façades, reducing their capacity of sunlight reflection. In this scenario, the present study analyzed the addition of different types of titanium dioxide, anatase and rutile, in cement tiles for building façades, combining the ease and speed of assembly with the self-cleaning effects of photocatalysis. The 1 cm thick tiles were produced with a 1:3 mortar ratio (cement:sand/dry aggregate) with a 0.5 water:cement ratio and the addition of 0.3% polypropylene fiber. Different admixture levels (0%, 5%, and 10%) of rutile and anatase titanium dioxide were used. The samples were tested for flexural strength, absorption, permeability, and photocatalysis effect by observing the color change and surface characteristics of the boards using a spectrophotometer. In addition, the hygroscopicity was analyzed through a water drop, using a goniometer. The results obtained showed that cement tiles with 5% titanium dioxide, which influences the color variation of the tiles, meet the regulatory requirements for use in outside environments. Thus, these materials have the potential to be used as cool façades since, by keeping their color lighter, the materials can reflect sunlight, therefore keeping lower temperatures inside the building, and, consequently, minimizing the heat island effect.

Keywords: cool façades; titanium dioxide; photocatalysis; cement mortars

Citation: Qualharini, E.L.; Stolz, C.M.; Martini, M.; Polesello, E.; da Silva, C.R. Self-Cleaning Mortar Façades with Addition of Anatase and Rutile Titanium Dioxide for Cool Façades. *Energies* **2023**, *16*, 1874. https://doi.org/10.3390/en16041874

Academic Editors: Chi-Ming Lai and F. Pacheco Torgal

Received: 29 December 2022
Revised: 20 January 2023
Accepted: 4 February 2023
Published: 14 February 2023

1. Introduction

A report published by the United Nations [1] presented the perspective that two-thirds of the world's population will be living in metropolitan areas by 2050, thus aggravating urban concentration. As a result, the regional climate changes will intensify and there will be a greater necessity for innovative and higher-quality construction systems. Thus, the worldwide trend is that the impact of these characteristics, as decisive factors in the choice of systems, components, and elements, is increasing, and that is why the advancement of the engineering and architecture areas must be aligned with those requirements [2].

In this scenario, there are traditional buildings that need to be optimized, particularly their façades, since most of the coatings used in this area require constant maintenance, which, if not carried out, will wear out the aesthetic, structural, and even safety aspects of a building. In addition, buildings in urban environments quickly stain because of deposits of particulate matter, in addition to the quite common darkened contours [3]. Furthermore, the constant need for interventions in the building after its completion is a rework that does not match the global trends of optimized processes over façade systems that use cement tiles, including the use, by the construction sector nowadays, of nanomaterials because of their special properties that can provide greater durability, fire resistance, thermal stability, and self-cleaning. As for the last property, the application of self-cleaning agents as well as photocatalytic coatings on the surface of construction elements can reduce the degradation generated by the environment in which they are inserted [4]. The principle that guides the photocatalysis process is based on the transfer of electrons between the valence and conduction band layers, opening oxidizing empty spaces and releasing reducing electrons. This operation uses the characteristics of semiconductor materials, which have a gap between their valence and conduction layers. Upon receiving an excitation through irradiation, these materials present a decrease in this distance until eventually allowing the exchange of electrons from the valence layer to the conduction layer [5,6].

There are several chemical constituents such as metal oxides and sulfides whose addition can cause the reactions that allow the degradation of pollutants by photocatalysis due to their appropriate band gap and light absorption properties [7]. One of the main elements of these constituents is titanium dioxide (TiO_2), which is an admixture used with mortars, concrete, and coatings [8,9]. In the presence of UV rays for a certain time, the material generates oxygen voids and hydroxyl radicals, creating changes in the contact angle between the water droplets and the surface [7]. In an application with atmospheric exposure, after degradation of the pollutants, the hydrophilicity generated by the reaction to UV rays allows a superficial washing, since the water starts to percolate through the material, taking the pollutants with it.

Studies in the area, such as those presented in [3,9,10], make use of the anatase titanium dioxide. However, its availability in the Brazilian market is limited, which makes rutile titanium dioxide an alternative, especially as some authors, such as Poon and Chueng [11] and Ibrahim et al. [12], achieved good results with this material active in the photocatalysis process.

The photocatalytic coating resulting from the addition of TiO_2 can sustain sunlight reflectance of building façades, making it more advantageous by keeping their initial high values of sunlight reflectance for longer periods, in addition to preventing overheating of surfaces exposed to the sun. Importantly, these benefits decay over time due to exposure to the environment [4].

In view of the above characteristics, cement materials with TiO_2 are cold materials, which are generally defined as all materials or paints capable of keeping lower surface temperatures, compared to the traditional ones, absorbing and storing reduced amounts of sunlight radiation or increasing water evaporation [13].

According to Croce et al. [13], cold materials are characterized by high sunlight reflectivity and high infrared emissivity. Such functions help to lower the surface temperature, in this case, the façades, reducing the convection of heat from the site to the atmosphere and thus reducing the air temperature. Mansouri et al. [14] show that great interest was directed to surface materials, especially those that have high reflectivity, that is, high albedo to minimize the absorption of solar radiation and, therefore, reduce its restitution in long wavelengths at night.

Some research has already proven the positive effect of reflective materials in moderating the urban microclimate, and there is a gap as to their effect on the indoor environment and energy consumption of buildings.

Designers and architects tend to adopt a reduced palette of colors on building façades to benefit from the energy gains from their high sunlight reflectance. This feature can be increased with coatings in light or reflective colors applied to roofs, floors, or walls [15]. Yuxuan et al. explain that cold materials can contribute from 11% to 27% reduction in peak-hour cooling demand [16].

In this scenario, this paper aims at the production of cement tiles for façades, focusing on improving building thermal comfort with a mixture of two types of titanium dioxide

(TiO_2), the rutile and the anatase, in different contents, to achieve photocatalysis on the finished product, thus preserving the reflective characteristics designed for façades.

2. Materials and Methods

The experimental program was designed for identifying the effectiveness of photocatalysis when different percentages of titanium dioxide (TiO_2) are added to cement tiles. To this end, cement tiles were produced with two types of titanium dioxide admixtures, namely rutile and anatase, both at 5% and 10% ratios, besides the reference tiles, without TiO_2. The physical properties and the flexural strength of the produced materials were evaluated in the fresh and hardened states. The samples were subjected to the staining agents methylene blue and rhodamine B, and then they were exposed to ultraviolet and urban environments for curing. Finally, a water drop was subjected to readings of color variation and contact angle, as shown schematically in Figure 1.

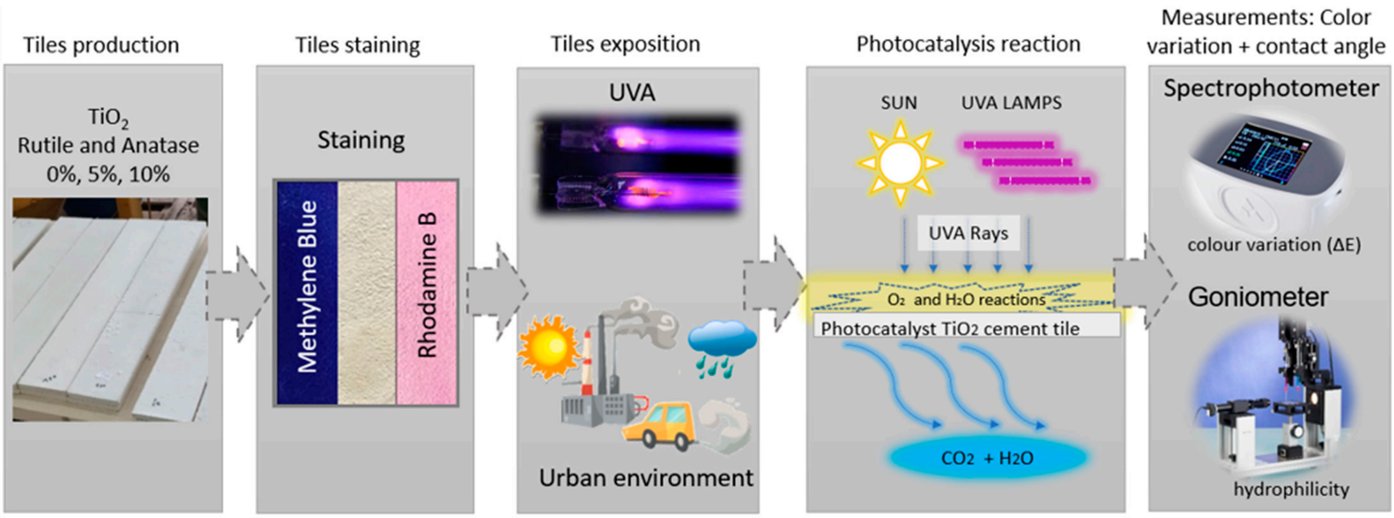

Figure 1. Schematic representation of the experimental program.

According to the ratios used by other studies, such as those of Jimenez-Relinque et al. [17] and Cárdenas et al. [18], the cement tiles were produced with a 1:3 ratio (cement:sand, dry materials, by volume, converted into mass) with a 0.5 water:cement ratio. The percentage of polypropylene fiber was set at 0.3%, as it showed an excellent viability in the study by Mohseni et al. [19], which used the same fiber type.

The percentages of titanium dioxide were adopted based on the choices and results of other studies, highlighting Cárdenas et al. [18], Diamanti et al. [20], and Shen et al. [21], and set at 0% for the standard sample and up to 5% and 10% of the amount of cement.

The thickness of the tiles was defined as 1.0 cm based on the thicknesses of cement tiles commonly available for external applications, made by Brazilian and international manufacturers such as INFIBRA [22], BRASILIT [23], and Valcan [24].

2.1. Materials

The production of cement tiles used CPB-40 white Portland cement, with a specific mass of 3.0 g/cm^3, according to the results obtained in laboratory tests. The properties of the cement are presented in Table 1, according to the manufacturer's information.

The small aggregate used to confer the white color to the tiles was fine white sand, commonly known as lagoon sand. The characterization of this material showed that the sand has a 1.03 fineness modulus, a 0.6 mm maximum characteristic dimension, and a 2.62 g/cm^3 of specific mass.

The polypropylene fiber used is 12 mm long and 18 µm in diameter, as shown in Figure 2. According to the manufacturer, its tensile strength is from 500 to 600 MPa, and its specific weight is 0.91 g/cm^3. Tap water coming from the municipal distribution network was used to produce the cement tiles.

Table 1. Properties of the CPB-40 white Portland cement.

Property	Results	NBR 16697-2018 Limits
Fire loss	≤5%	≤12%
Insoluble residue	≤5%	≤3.5%
Sulfate content	≤4%	≤4%
Chloride content	≤0.1%	≤0.1%
Set time	≥45 min	≥60 min
Expandability	≤10 mm	≤5 mm
Compressive strength—2 days	>37 MPa	>15 MPa
Compressive strength—28 days	≥60 MPa	≥40 MPa

Note: Manufacturer information.

Figure 2. Dimensions and visual appearance of the polypropylene fiber used in the study.

The anatase and rutile titanium dioxides used in the manufacturing process were purchased in powder, the main characteristics of which can be seen in Table 2, as provided by the manufacturer.

Table 2. Properties of the anatase and rutile titanium dioxide.

Physical–Chemical Characteristics	Anatase	Rutile
Titanium dioxide concentration (%)	99.10	96.3
Evaporated material (%, 105 °C)	0.20	0.26
pH in aqueous solution	7.7	7.3
Oil absorption (g/100 g)	24	19.2
Fineness (% retained on a 45 µm sieve)	0.03	0.05

To obtain the adequate workability of the mortar to produce the boards, a superplasticizer additive was used, based on the chemical polycarboxylate, with a density between 1.067 and 1.107 g/cm^3, pH between 5.0 and 7.0, and solids between 38% and 42%.

2.2. Methodology of Tests Performed

The production of mortars followed a mixing methodology adapted from the NBR 7215 [25]. The fibers were manually dispersed and mixed with the sand, while the titanium dioxide was mixed with water and kept in constant movement until its use. First, cement and water with TiO_2 were added to the mortar mixer and then mixed for 30 s at low speed. Then, the sand with the fibers was added to the mixture during a period of 30 s, as indicated by the standard, followed by a 90 s rest, and then went through a final 60 s mixing at high speed.

In the fresh state, the mortars were characterized according to their consistency index, so that the superplasticizer admixture content was dosed in amounts between 13 g and 13.5 g so that they reached values between 260 mm $\pm$ 5 mm, as indicated by the NBR 13276 [26]. The mass density in the fresh state was carried out following the provisions of the NBR 13278 standard [27].

The molding of specimens for carrying out the tests in the hardened state was carried out in wooden molds painted with gray acrylic paint to reduce water absorption. The dimensions of the specimens followed the determinations of current regulations: $60 \times 10 \times 1$ cm^3 for permeability, $22 \times 10 \times 1$ cm^3 for flexural strength, and $10 \times 10 \times 1$ cm^3 for the other ones. After molding, the specimens were kept in the molds for three days until they were demolded.

Tests carried out on the hardened cement tiles followed the NBR 15498 standard [28]. The specimens used followed the minimum dimensions recommended by the norm for standard procedures, and three samples were molded for each of the analyses carried out, making it possible to perform a comparative average. The tests carried out in accordance with this standard were flexural tensile strength, water absorption, permeability, and dimensional variation, all at 30 days of age, due to the availability of equipment for their realization.

The flexural tensile strength test was carried out in the unsaturated state, cured at a temperature of 23 $\pm$ 10 °C and relative humidity of 50 $\pm$ 20%, and the saturated state, stored for 24 h immersed in water.

To evaluate the photocatalysis, staining tests were performed and the contact angle of a water drop on the samples was measured.

For the staining test, the rhodamine B admixture was used, as indicated by the international standard UNI 11259 [29], and methylene blue was used, as indicated by the ASTM C1378 standard [30]. According to the use by similar studies, such as those of Pozo-Antonio and Dionisio [3] and Rosales et al. [31], 0.5 g/L rhodamine B and 1% methylene blue concentrations were defined. The admixtures were applied with a syringe in an amount of 0.5 mL of each substance in each specimen. To ensure uniform dispersion throughout the material, the liquid was spread over the analysis region with a brush.

For comparative purposes, each specimen was divided into three strips of the same size; the substances for staining were applied to two of them, and the third was used as a reference, without staining. Figure 3 exemplifies the staining of the tiles.

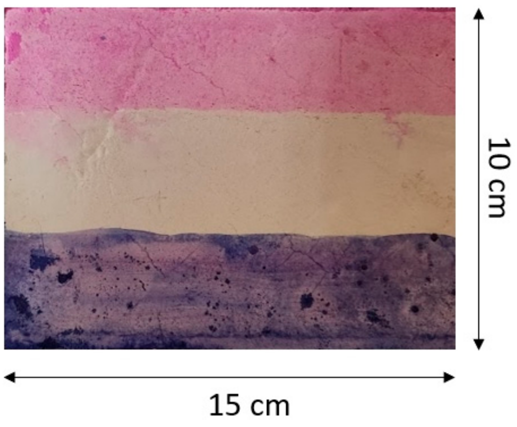

Figure 3. Tiles stained by rhodamine B and methylene blue.

After staining, the specimens were subjected to different exposure environments. Some of the specimens were taken to a chamber completely sealed from UVA radiation, containing six USHIO 30 W lamps and a 365 nm peak wavelength (Figure 4), and some of the specimens were exposed to the open air, in an urban environment and close to the flow of vehicles (Figure 5). They were arranged in a position with constant sunlight incidence, with the chosen angle of inclination (0°).

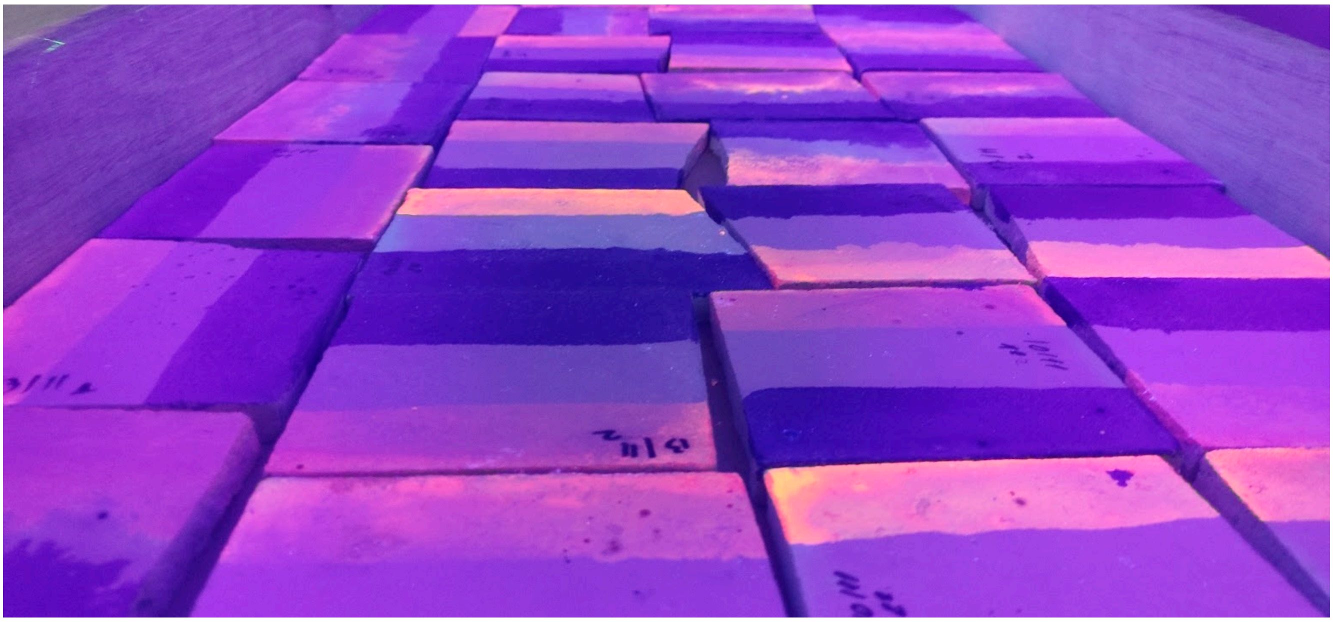

Figure 4. Tiles stained by rhodamine B and methylene blue exposed to UVA radiation.

Figure 5. Tiles stained by rhodamine B and methylene blue exposed to the urban environment.

Exposure to UVA radiation is justified by the fact that photocatalysis, unlike wetting, is not based only on repelling dirt with water, but rather on reacting with UV radiation from sunlight [20] so that there is a decomposition of pollutants that deposit on the tile.

Changes in color of the tiles exposed to UVA radiation were analyzed before exposure and after 46 h of exposure, due to equipment availability times. The tiles exposed to the urban environment were submitted to measurements at 0 and 49 days, being limited to this maximum period according to the availability of equipment.

The spectrophotometer used was a Delta Vista brand, model 450 G, with 45/0° optical geometry. The number of measurements per stain remained constant, with 3 measurement points on each substance and 3 measurements on the reference range. To standardize the color measurement points and to ensure that the readings were always performed in the same place on the tiles, a template was made in a 3D printer with the opening of the equipment used, allowing accuracy and guaranteeing that the same points were analyzed in each reading. Figure 6 shows the reading being performed on one of the specimens, with the spectrophotometer using the printed support.

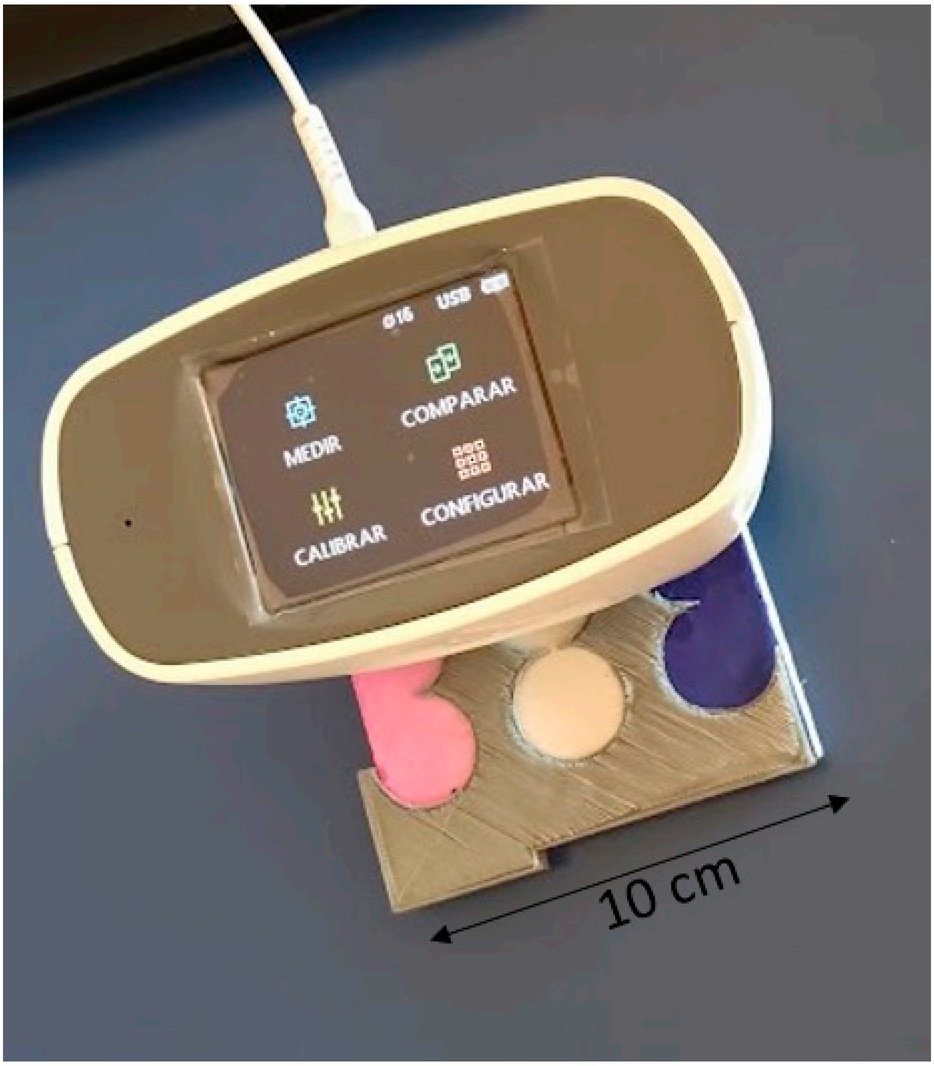

Figure 6. Color measurement with spectrophotometer using template for standardization.

The results obtained through measurements with the equipment convert the coloring to numerical format, in the CIELAB system. This system has three axes, like a coordinate system, in which the vertical axis (L) is represented in an increasing way from black to white, and the axes of the horizontal plane are represented by the variations from green to red (a) and from the blue to yellow (b). The difference between the colors obtained in the $L \times a \times b$ coordinates at two different times is given through the color variation (ΔE), a property that will be used to compare the staining of the cement tiles.

To measure the contact angle, the Dataphysics OCA15EC goniometer equipment was used. The test consists of observing and measuring the contact angle formed by a water drop when it falls on the study tile. The contact angle was analyzed in two moments: in an initial reading, and after irradiating the tile in a UV chamber for periods of 22 h.

The analysis of results was performed using analysis of variance, in the Statistica software, version 10, with 95% reliability, in order to assess whether the response variables were statistically influenced by the controllable variables.

For a visual qualitative analysis of the distribution of TiO_2 in the cementitious matrix and aiming to analyze the interaction of the paste with the fibers and the behavior of the composite as a whole, images of scanning electronic microscopy (SEM) were obtained, using a JEOL JSM-6510LV instrument.

3. Results

To facilitate the presentation of results, the following nomenclature will be used for cement tiles: REF, for reference; 5A and 10A for 5% and 10% TiO_2 anatase admixtures, respectively; and 5R and 10R, for 5% and 10% TiO_2 rutile admixtures, respectively.

In the fresh state, the density of the mortar with which the tiles were produced was determined, verifying that all mixtures presented density values between 2.01 and 2.08 g/cm^3, demonstrating that the titanium dioxide admixture did not seem to have influenced this property of the material.

Table 3 presents the average results of three determinations obtained in the tests in the hardened state of the cement tiles.

Table 3. Physical properties and flexural strength of cement tiles produced with different contents of anatase and rutile titanium dioxide.

Cement Tile	Permeability (Qualitative)	Dimensional Variation (mm/m)		Water Absorption (%)	Flexural Tensile Strength (MPa)	
		X Axis	Y Axis		Not Saturated	Saturated
REF	Moisture	2.49	2.90	7.17	4.27	4.06
5A	Not present	2.02	1.94	6.08	4.15	4.04
10A	Not present	2.12	2.90	6.11	3.91	3.27
5R	Not present	3.02	2.86	6.67	4.25	4.12
10R	Not present	2.84	3.19	6.52	3.42	3.16

The permeability test is carried out by analyzing the underside of the tile exposed to a layer of water, which, for positive results, must not show drop formation, but may show signs of moisture. All cement tiles were approved in terms of permeability, as none showed drop formation ("not present"). Only the reference tile, without the TiO_2 admixture, showed "moisture" marks on the side opposite to contact with water, indicating the improvement in the efficiency of the tiles with the admixture, in terms of their tightness.

As for dimensional variation, the regulations do not have limits; however, it is observed that in the Brazilian market, the range of dimensional variation is between 2.0 and 2.7 mm/m, BRASILIT [23] and INFIBRA [22]. Thus, it appears that the cement tiles with the greatest variations were those produced with rutile titanium dioxide, reaching values above 3 mm/m.

As for water absorption, it appears that the addition of TiO_2 reduced absorption, most likely due to the presence of finer substances that help to close capillary pores. The anatase titanium dioxide admixture decreased water absorption more, compared to rutile, most likely due to its greater fineness.

As for the average flexural tensile strength of the specimens, there was a greater reduction in tile strength with 10% rutile admixture (10R), with a reduction of approximately 20% in flexural tensile strength, in relation to the reference in the saturated and unsaturated states. Considering the criteria in the NBR 15498 [28], cement tiles must have at least 4 MPa of flexural tensile strength, so the tiles with 10% TiO_2 admixture do not meet this requirement. Thus, the ideal would be to use a maximum of 5% admixture.

After the flexural tensile strength testing, the samples were submitted to a qualitative visual analysis of the distribution of TiO_2 and fibers in the cementitious matrix. These scanning electron microscopy (SEM) images, with 50× magnification, are shown in Figure 7a–e. The SEM images with 50× magnification made it possible to observe that in the reference sample (6a) there was an agglomeration of fine aggregate, indicating a lack of paste in the composite. The images with the presence of TiO_2 rutile and anatase showed a homogeneous matrix without the presence of agglomerates, which indicates a good dispersion of the compound. Some pores were evident in the samples, and it was possible to observe in all of them that there was no agglomeration of fibers.

3.1. Photocatalysis Analysis

This item presents the results of staining analyses using a spectrophotometer, in all study conditions.

The cement tiles were stained with rhodamine B and methylene blue and then exposed to the urban environment and UVA radiation. Color variation (ΔE) of the tiles was evaluated using a spectrophotometer. The tiles exposed to UVA radiation were analyzed before exposure (0 h) and after 46 h of exposure. The tiles exposed to the urban environment were subjected to measurements at 0 and 49 days.

The spectrophotometer ΔE reading results, comparing the color at time zero with the color at the final reading, are fully presented in Appendix A, Tables A1 and A2. With these results, a 95% confidence analysis on variance was carried out with the Statistica 10 Software, in which verification of the influence of the titanium dioxide levels and the curing and staining conditions of the cement tiles on the ΔE was performed.

3.1.1. Cement Tiles Exposed to the Urban Environment

Firstly, the color variations of cement tiles exposed to the urban environment will be presented, with an evaluation of color variation (ΔE) from day zero of exposure to the last day of exposure (day 49). Table 4 presents the main effects analysis of variance for the tiles produced with TiO_2 rutile and anatase, with and without methylene blue staining, and cured in an urban environment over time.

Table 4. Main effects analysis of variance for tiles produced with TiO_2 rutile and anatase, with and without methylene blue staining, cured in an urban environment over time.

TiO_2	Variable	SS	DF	MS	Fcalc	p-Factor	Significative
Rutile	Staining	15,714.69	1	15,714.69	7035.721	0.000000	Yes
	TiO_2 (%)	23.56	2	11.78	5.273	0.019635	Yes
	Error	31.27	14	2.23			
Anatase	Staining	15,234.43	1	15,234.43	1927.017	0.000000	Yes
	TiO_2 (%)	75.50	2	37.75	4.775	0.026243	Yes
	Error	110.68	14	7.91			

SS: sum of squares, DF: degrees of freedom, MS: mean squares; Fcalc: calculated F-value.

This analysis showed that the presence of methylene blue staining and the content of TiO_2 rutile and anatase were significant in color variation over time. This behavior can be better visualized in Figure 8, which shows that the higher the TiO_2 rutile content (Figure 8a), the greater the color variation observed in the tiles stained with methylene blue. Figure 8b shows that TiO_2 anatase was efficient only with a higher content, 10%, regarding color variation. This fact suggests a greater efficiency of TiO_2 rutile with lower contents, compared to anatase.

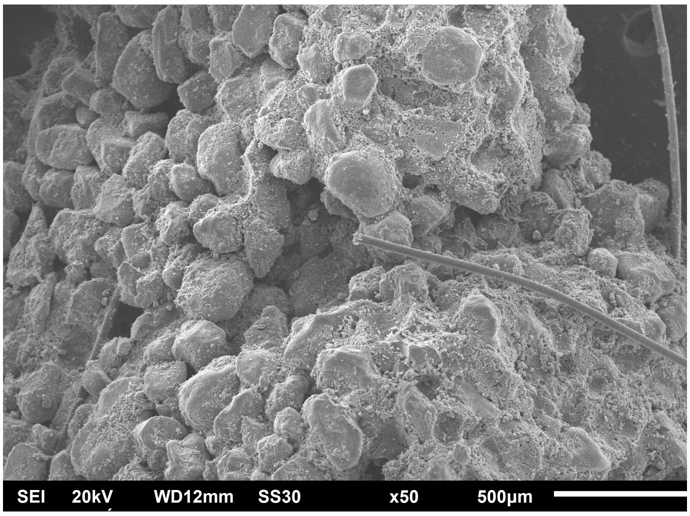

(**a**) REF

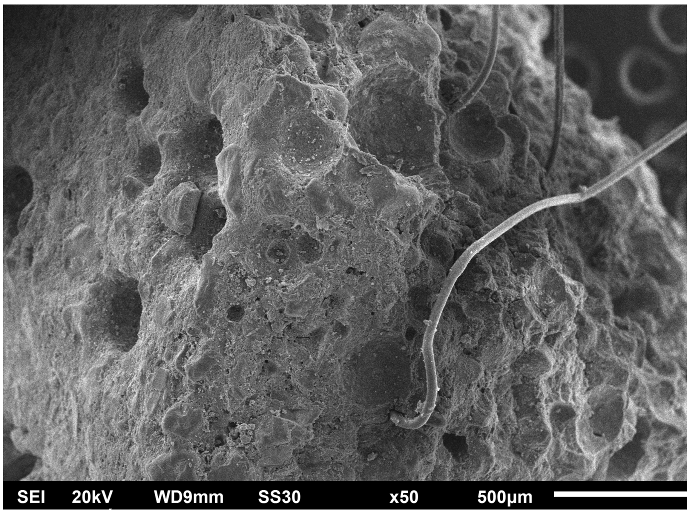

(**b**) 5R

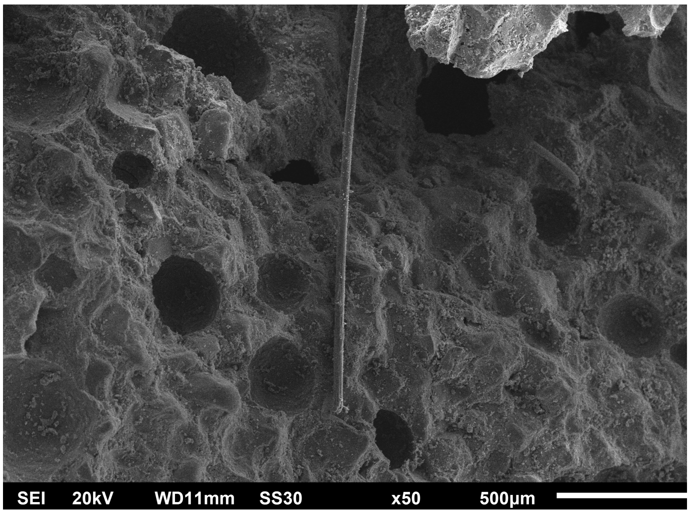

(**c**) 10R

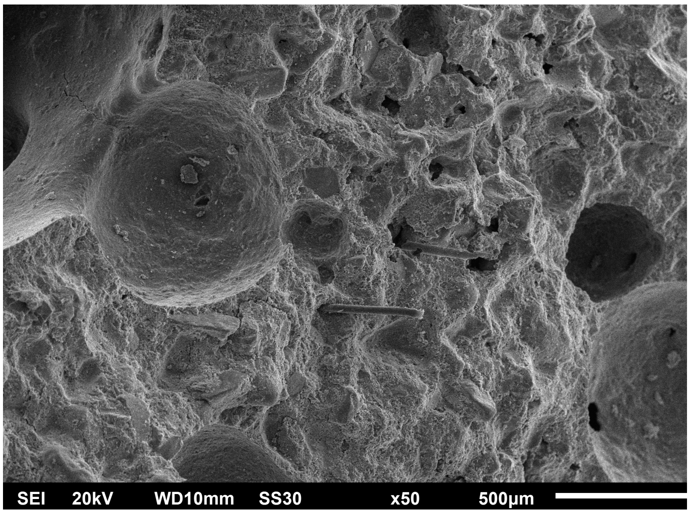

(**d**) 5A

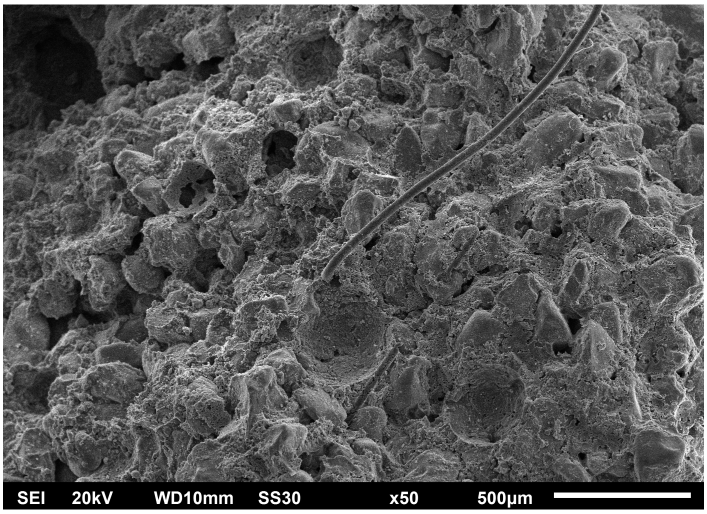

(**e**) 10A

Figure 7. Scanning electron microscopy (SEM) images, with 50x magnification: (**a**) REF, (**b**) 5R, (**c**) 10R, (**d**) 5A, (**e**) 10A.

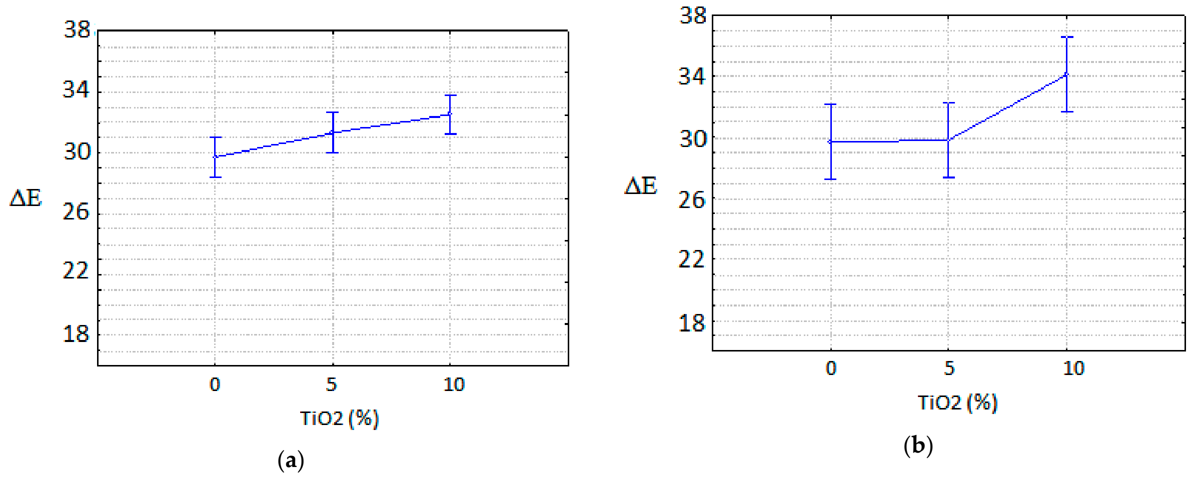

Figure 8. Analysis of the influence of TiO_2 content, with and without staining by methylene blue, cured in an urban environment over time: (**a**) rutile, (**b**) anatase.

Table 5 presents the main effects analysis of variance for the tiles produced with rutile TiO_2, with and without staining by rhodamine B, and submitted to curing in an urban environment over time. The color variation (ΔE) from day zero of exposure to the last day of exposure (49) was evaluated.

Table 5. Main effects analysis of variance for tiles produced with TiO_2 rutile and anatase, with and without staining by rhodamine B, cured in an urban environment over time.

TiO_2	Variable	SS	DF	MS	Fcalc	p-Factor	Significative
Rutile	Staining	7906.950	1	7906.950	922.301	0.000000	Yes
	TiO_2 (%)	67.882	2	33.941	3.959	0.043379	Yes
	Error	120.023	14	8.573			
Anatase	Staining	8534.28	1	8534.28	941.792	0.000000	Yes
	TiO_2 (%)	45.23	2	22.62	2.496	0.118295	No
	Error	126.86	14	9.06			

SS: sum of squares, DF: degrees of freedom, MS: mean squares; Fcalc: calculated F-value.

Table 6 and Figure 9, presented below, show that there was a significant influence of rutile TiO_2 (Figure 9a), with no influence of anatase content (Figure 9b), on the staining and color variation of the tiles. Thus, it appears that the TiO_2 anatase content was not significant in the color variation of the tiles stained by rhodamine B; i.e., it was not beneficial for their self-cleaning characteristic.

Table 6. Visual aspect of cement tiles, before and after exposure to the urban environment, per different stains and TiO_2 contents.

	No Staining	Methylene Blue	Rhodamine B
REF	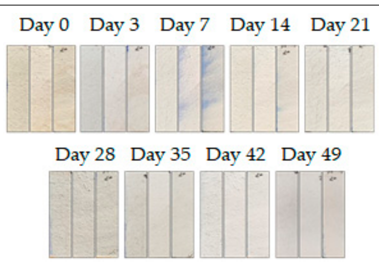	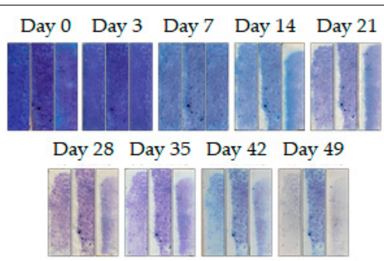	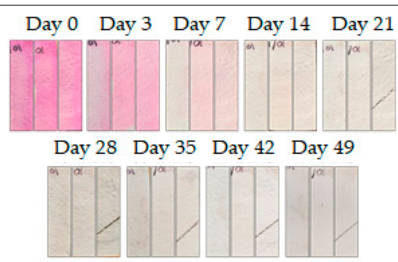

Table 6. *Cont.*

	No Staining	Methylene Blue	Rhodamine B
5A	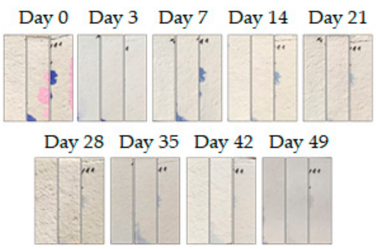	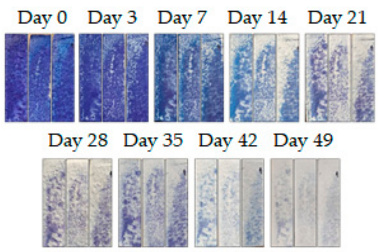	
10A	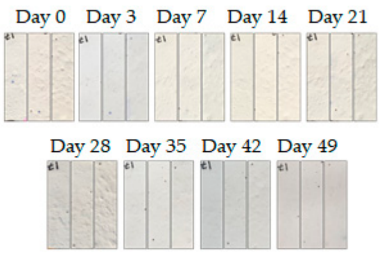	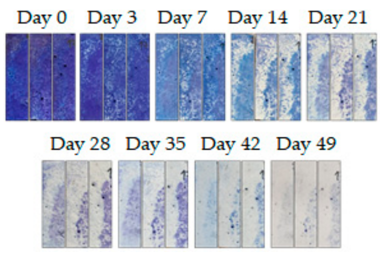	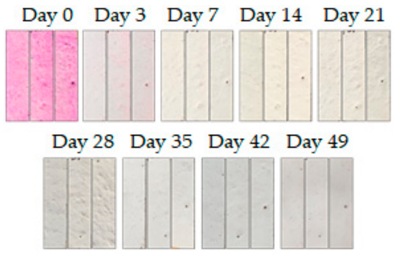
5R		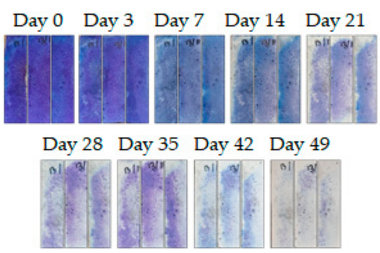	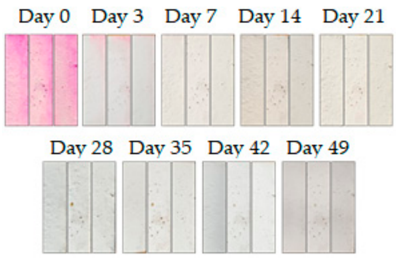
10R	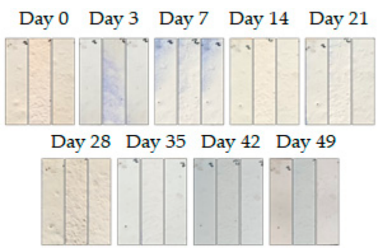	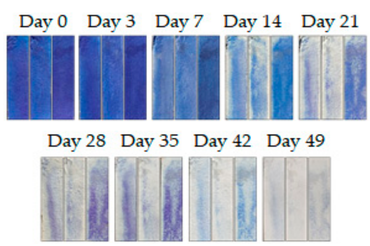	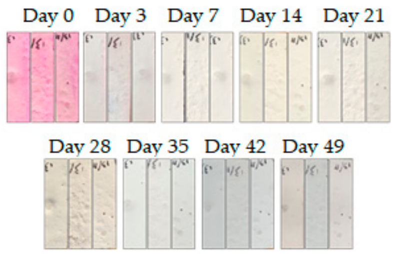

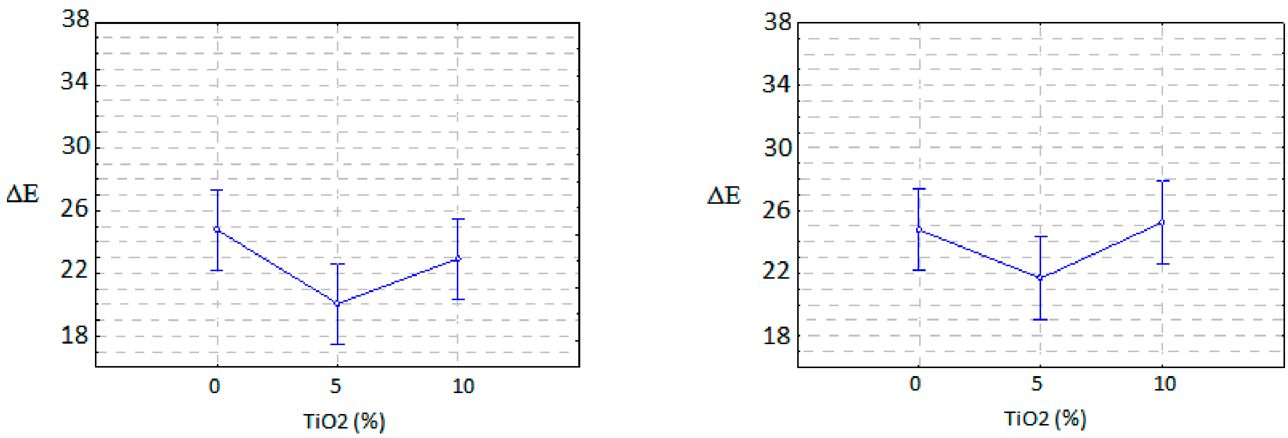

(**a**) (**b**)

Figure 9. Analysis of the influence of TiO_2 content, with and without staining by rhodamine B, cured in an urban environment over time: (**a**) rutile, (**b**) anatase.

The images in Table 6 show the visual aspect of the cement tiles, before and after exposure to the urban environment, per the different stains and TiO_2 contents.

Comparing the images, it is possible to see that methylene blue was more resistant to being removed from the plates than rhodamine B. This fact was reflected in the results of color variation read by the spectrophotometer.

For the reference specimens, without any type of TiO_2, it is possible to observe that the stains were more resistant to being removed, and even rhodamine is visually visible until the 14th day and methylene blue is very evident until the 49th day. These facts underscore the efficiency of the presence of titanium dioxide in the self-cleaning effect of cementitious tiles.

3.1.2. Cement Tiles Exposed to a UVA Chamber

This section will present the color variations, which were evaluated before exposure and after 46 h of exposure, of cement tiles exposed to UVA radiation. Table 7 presents the main effects analysis of variance on the tiles produced with TiO_2 rutile and anatase, with and without staining by methylene blue, and subjected to UVA radiation.

Table 7. Main effects analysis of variance on tiles produced with TiO_2 rutile and anatase, with and without staining by methylene blue, subjected to UVA radiation.

TiO_2	Variable	SS	DGF	MS	F	p-Factor	Significative
Rutile	Staining	157.8325	1	157.8325	10.24568	0.012596	Yes
	TiO_2 (%)	21.0350	2	10.5175	0.68274	0.532401	No
	Error	123.2384	8	15.4048			
Anatase	Staining	196.9920	1	196.9920	11.63158	0.009216	Yes
	TiO_2 (%)	10.8912	2	5.4456	0.32154	0.733982	No
	Error	135.4877	8	16.9360			

Table 8 presents the main effects analysis of variance on the tiles produced with TiO_2 rutile and anatase, with and without staining by rhodamine B, and submitted to UVA radiation.

Table 8. Main effects analysis of variance on tiles produced with TiO_2 rutile and anatase, with and without staining by rhodamine B, subjected to UVA radiation.

TiO_2	Variable	SS	DGF	MS	F	p-Factor	Significative
Rutile	Staining	717.963	1	717.963	35.15020	0.000350	Yes
	TiO_2 (%)	122.690	2	61.345	3.00336	0.106418	No
	Error	163.405	8	20.426			
Anatase	Staining	626.8411	1	626.8411	40.55731	0.000216	Yes
	TiO_2 (%)	82.7245	2	41.3623	2.67618	0.128863	No
	Error	123.6455	8	15.4557			

It is observed that, when 46 tiles were exposed to the UVA radiation in a chamber, the color variation on the analyzed tiles was not influenced by the TiO_2 content in their composition.

The images in Table 9 show the visual aspect of the cement tiles, before and after exposure to the urban environment, per different stains and TiO_2 contents.

Table 9. Visual appearance of cement tiles, before and after exposure to UVA radiation, per different stains and TiO_2 contents.

	REF		**5A**		**10A**		**5R**		**10R**	
	0 h	**48 h**	**0 h**	**48 h**	**0 h**	**48 h**	**0 h**	**48 h**	**0 h**	**48 h**
No staining	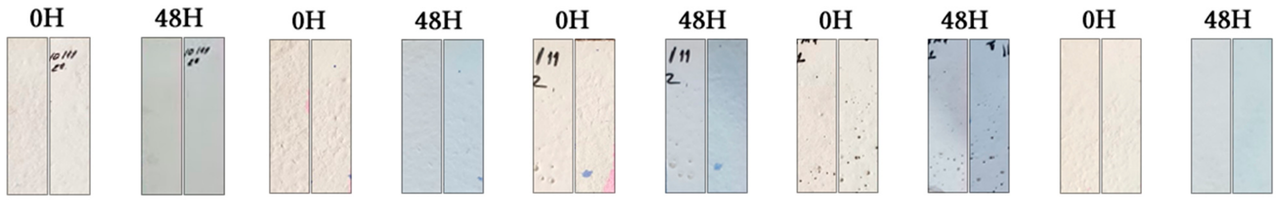									
Methylene blue	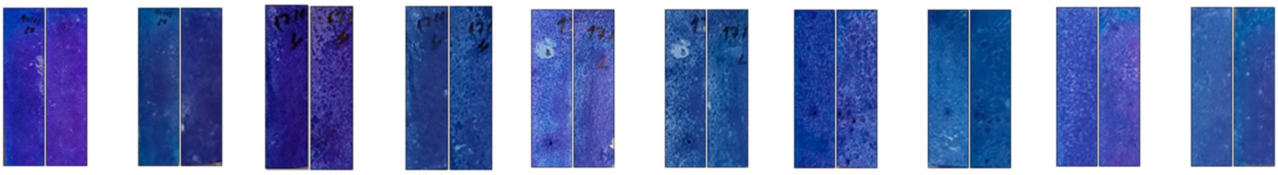									
Rhodamine B	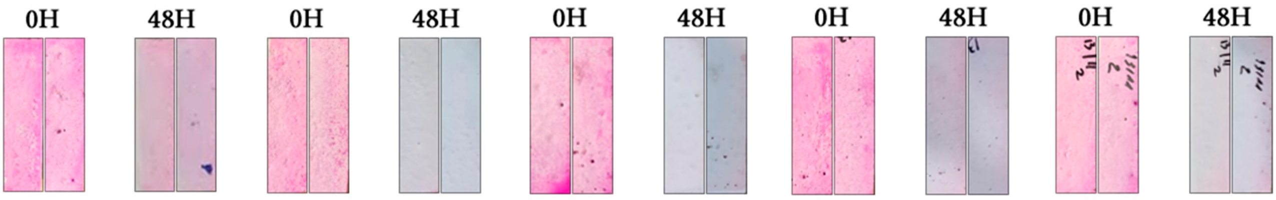									

Confirming what was presented in the statistical analysis, the images presented in Table 8 show that there was no great reduction in coloration with different levels of TiO_2. It is observed that all samples stained with methylene blue showed a small reduction in color, while those stained with rhodamine B showed a greater loss of color, which was not enough to completely eliminate the pink color of the staining agent.

3.1.3. Evaluation of the Superficial Tension through Contact Angle

The contact angle tests were performed on aged (submerged in hot water for 56 days) and non-aged specimens, for comparative effects of the hydrophilicity of the samples.

The same procedures were performed after 24 h from the exposure to a 365 nm wavelength UVA light, to verify if the contact angle would have any alteration. The mean results regarding the contact angles and their drop-wetting visualization are shown in Table 10.

Table 10. Contact angle of a water drop on the surface of a cement tile, before and after application of UVA light, under air conditioned curing and accelerated aging.

CP	**Initial Reading (°)**		**Reading after Application of UVA Light (°)**	
	Air Conditioned	**Aged**	**Air Conditioned**	**Aged**
REF	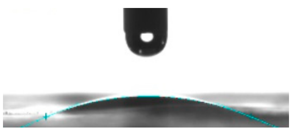 22.05	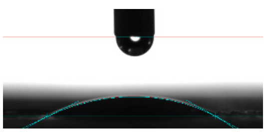 27.25	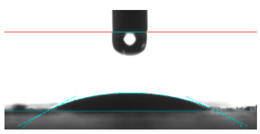 26.35	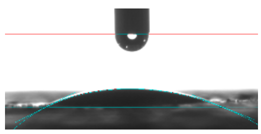 24.20

Table 10. *Cont.*

CP	Initial Reading (°)		Reading after Application of UVA Light (°)	
	Air Conditioned	**Aged**	**Air Conditioned**	**Aged**
5R	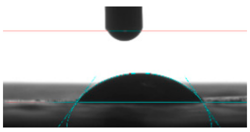 53.90	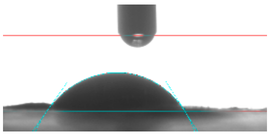 55.80	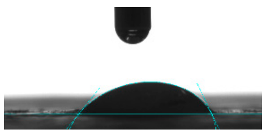 57.95	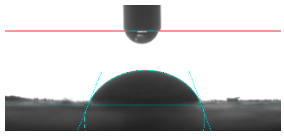 68.95
10R	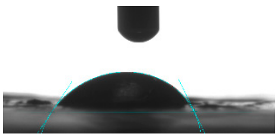 59.95	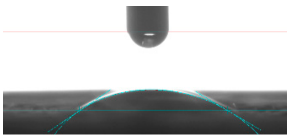 32.30	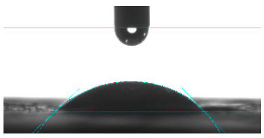 44.20	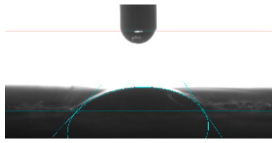 50.70
5A	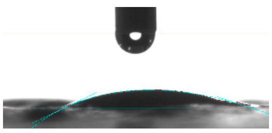 21.60	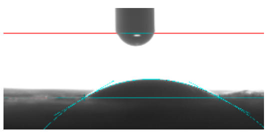 28.90	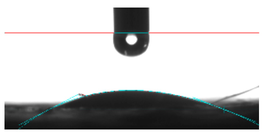 24.25	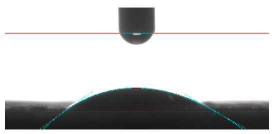 32.75
10A	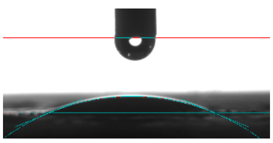 22.40	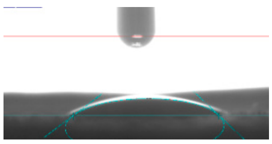 40.05	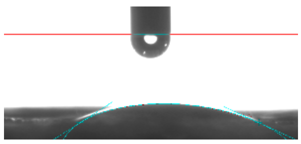 28.60	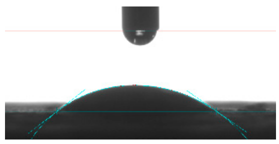 36.25

All results were in the range considered hydrophilic, i.e., less than 90°. This is excellent for working with photocatalysis because it allows the superficially accumulated dirt to be washed off. However, a more than 200% increase is observed in the contact angle of the tiles with TiO_2 rutile in their composition, compared to the reference tiles. This may be an indication of changes in the surface tension of the tiles with an increased admixture of TiO_2 rutile in their composition, which may impair the rolling of water droplets.

4. Discussion

The results of the tests of flexural strength efforts showed that the cement tiles with a 10% TiO_2 admixture were the ones that presented the lowest flexural tensile strength, with up to 20% reduction, whereas the rutile showed the larger reductions. The tiles' water absorption was reduced by the TiO_2, when compared to the reference tiles, and the permeability was within the expected range, without the formation of water droplets.

When analyzing the staining of the tiles, it was verified that the methylene blue was more effective in demonstrating the efficiency of TiO_2 than the rhodamine B. This is probably related to a greater color contrast of the methylene blue with the reference tile. As for the stains by methylene blue, it was observed that the presence of TiO_2 was significant in the color variation after the tiles were exposed to the urban environment, thus demonstrating that environmental factors, such as rain, can corroborate the efficiency of maintenance of the tile color.

It was verified that there is a direct relationship between the rutile TiO_2 content and the color variation. An increase in its addition caused a decrease in the staining; i.e., a 5% admixture reduced the staining on the tiles, and 10% admixture reduced the staining even more. The anatase, on the other hand, did not show a significant influence at 5% admixture, but a 10% admixture showed a significant influence on the staining reduction, showing a greater difference in color in contrast with the reference tiles without the TiO_2 admixture.

When the samples were exposed to UVA radiation, it was not possible to observe the influence of TiO_2 contents in their composition on color variation. This may have occurred due to the absence of running water (rainwater, for example) to carry away the particles. In this way, the UVA radiation reactive particles remained on the tiles.

It was observed that, with the TiO_2 admixture, the reflectance and/or emittance of the tiles were preserved because of the staining reduction in contrast with the reference tiles, thus preserving the initial color of the surface, which leads to a lower temperature of the tiles and, therefore, of the place where they are installed.

5. Conclusions

The present study evaluated the influence of TiO_2 rutile and anatase, both at 5% and 10%, on the self-cleaning capacity and on the photocatalysis of cement tiles for façades, focusing on the color maintenance and, consequently, on the sunlight reflection.

It was observed, at the end of the study, that these admixtures, up to 5% of the cement mortar, contributed to reaching the normative criteria for the flexural strength of the cement tiles and had a positive impact on the color variation of the tiles when submitted to the staining agent methylene blue and exposed to the urban environment. This fact positively influences the self-cleaning capacity of façades, and thus its capability of reducing stains helps to keep the façades cleaner, with lighter colors, benefiting the thermal comfort of the building and its surroundings.

As shown in the literature review, lighter colors have a greater capacity of reflecting sunlight, thus helping to reduce the temperature of the façades and, consequently, reducing the air temperature, contributing to mitigating the effects of urban heat islands.

Therefore, as a novel contribution, the present study states that the use of cement tiles with 5% rutile or anatase titanium dioxide can be beneficial for greater energy efficiency in buildings, contributing to their internal and external comfort, in addition to reducing maintenance and cleaning costs of buildings.

Author Contributions: Conceptualization, C.R.d.S.; methodology, M.M.; formal analysis, M.M. and C.M.S.; data curation, C.M.S. and E.P.; writing—original draft preparation, C.R.d.S. and C.M.S.; writing—review and editing, C.R.d.S., E.L.Q. and C.M.S.; supervision, E.L.Q., E.P. and C.M.S.; project administration, E.L.Q. and C.M.S. All authors have read and agreed to the published version of the manuscript.

Funding: This study was partly financed by the Coordenação de Aperfeiçoamento de Pessoal de Nível Superior—Brasil (CAPES)—Finance Code 001.

Data Availability Statement: Not applicable.

Acknowledgments: The authors would like to thank the Universidade FEEVALE and the Escola Politécnica of Universidade Federal do Rio de Janeiro for technical support and physical space for the experimental program execution and the analysis of results.

Conflicts of Interest: The authors declare no conflict of interest.

Appendix A

Table A1. Color variation of cement tiles after UVA curing.

		UVA Cure					
		Sample	**CP**	**ΔE Point 1**	**ΔE Point 2**	**ΔE Point 3**	**Average ΔE**
Reference	UVA	REF	CP1	−1.20	−0.25	−0.66	1.39
	UVA	REF	CP2	−3.63	0.31	0.34	3.66
	UVA	5R	CP1	−1.43	−0.97	−0.45	1.79
	UVA	5R	CP2	−0.85	−0.25	0.61	1.08
	UVA	10R	CP1	−0.63	0.27	0.88	1.12

Table A1. *Cont.*

	UVA Cure						
		Sample	**CP**	**ΔE Point 1**	**ΔE Point 2**	**ΔE Point 3**	**Average ΔE**
Reference	UVA	10R	CP2	−0.10	0.93	2.86	3.01
	UVA	5A	CP1	−1.31	−0.24	0.04	1.34
	UVA	5A	CP2	−2.49	0.47	0.79	2.66
	UVA	10A	CP1	0.04	−0.35	0.11	0.37
	UVA	10A	CP2	1.40	−0.46	0.13	1.48
Methylene blue	UVA	REF	CP1	0.46	−3.11	3.75	4.89
	UVA	REF	CP2	5.75	−14.16	8.92	17.70
	UVA	5R	CP1	0.35	−1.92	4.75	5.14
	UVA	5R	CP2	−1.24	−1.42	6.98	7.23
	UVA	10R	CP1	1.43	−3.98	5.30	6.78
	UVA	10R	CP2	5.53	−7.73	10.05	13.83
	UVA	5A	CP1	0.90	−2.12	4.57	5.11
	UVA	5A	CP2	2.62	−4.07	7.97	9.32
	UVA	10A	CP1	1.69	−3.07	6.73	7.59
	UVA	10A	CP2	9.40	−4.26	10.77	14.91
Rhodamine B	UVA	REF	CP1	2.75	−5.59	5.81	8.52
	UVA	REF	CP2	1.08	−3.03	7.07	7.77
	UVA	5R	CP1	6.60	−21.52	11.06	25.08
	UVA	5R	CP2	6.06	−19.24	11.72	23.33
	UVA	10R	CP1	6.34	−17.12	9.03	20.37
	UVA	10R	CP2	5.39	−15.91	10.48	19.80
	UVA	5A	CP1	5.09	−18.53	6.94	20.43
	UVA	5A	CP2	4.03	−17.71	7.78	19.76
	UVA	10A	CP1	4.47	−17.65	8.14	19.95
	UVA	10A	CP2	7.99	−18.43	6.78	21.20

Table A2. Color variation of cement tiles after exposure to an urban environment.

	Curing in an Urban Environment					
	Sample	**CP**	**ΔE Point 1**	**ΔE Point 2**	**ΔE Point 3**	**Average ΔE**
Reference	REF	CP1	1.03	1.27	1.45	1.25
	REF	CP2	0.70	0.81	1.58	1.03
	REF	CP3	2.41	2.06	2.15	2.21
	5R	CP1	0.56	0.33	0.50	0.46
	5R	CP2	1.41	0.57	0.48	0.82
	5R	CP3	0.76	0.48	0.95	0.73
	10R	CP1	1.98	3.97	4.08	3.34
	10R	CP2	1.46	3.72	2.07	2.42
	10R	CP3	1.34	2.67	3.40	2.47
	5A	CP1	9.19	0.86	5.47	5.17
	5A	CP2	0.44	2.13	5.18	2.58

Table A2. *Cont.*

Curing in an Urban Environment						
	Sample	**CP**	**ΔE Point 1**	**ΔE Point 2**	**ΔE Point 3**	**Average ΔE**
Reference	5A	CP3	0.47	0.17	2.87	1.17
	10A	CP1	2.12	1.94	1.90	1.99
	10A	CP2	1.87	2.68	1.24	1.93
	10A	CP3	1.22	2.65	1.82	1.89
Methylene blue	REF	CP1	54.34	61.47	56.15	57.32
	REF	CP2	53.24	64.70	56.18	58.04
	REF	CP3	58.46	61.60	55.40	58.49
	5R	CP1	63.38	65.48	60.25	63.04
	5R	CP2	51.52	62.43	64.04	59.33
	5R	CP3	66.25	58.67	65.55	63.49
	10R	CP1	58.22	57.57	72.16	62.65
	10R	CP2	59.16	59.15	69.68	62.66
	10R	CP3	65.36	55.69	63.62	61.56
	5A	CP1	50.06	61.75	56.34	56.05
	5A	CP2	53.22	59.03	60.30	57.52
	5A	CP3	58.74	46.23	64.63	56.53
	10A	CP1	64.79	67.99	67.44	66.74
	10A	CP2	67.05	67.80	69.36	68.07
	10A	CP3	58.68	64.35	69.34	64.12
Rhodamine B	REF	CP1	47.37	54.79	47.74	49.97
	REF	CP2	45.28	52.71	47.41	48.46
	REF	CP3	44.29	47.81	45.27	45.79
	5R	CP1	34.10	34.02	38.39	35.50
	5R	CP2	39.12	35.51	38.01	37.55
	5R	CP3	41.90	44.50	49.58	45.33
	10R	CP1	41.12	39.54	45.92	42.19
	10R	CP2	45.21	46.82	42.91	44.98
	10R	CP3	42.32	41.32	43.02	42.22
	5A	CP1	37.08	43.23	40.35	40.22
	5A	CP2	37.39	39.24	38.25	38.29
	5A	CP3	44.94	43.57	39.52	42.68
	10A	CP1	50.17	43.83	44.16	46.06
	10A	CP2	52.16	51.92	50.29	51.46
	10A	CP3	51.93	45.94	46.81	48.23

References

1. UN (United Nations). Sustainable Cities and Human Settlements. Available online: https://sdgs.un.org/topics/sustainable-cities-and-human-settlements (accessed on 20 December 2022).
2. Yi, Y.K. Building Facade Multi-Objective Optimization for Daylight and Aesthetical Perception. *Build. Environ.* **2019**, *156*, 178–190. [CrossRef]
3. Pozo-Antonio, J.S.; Dionísio, A. Self-Cleaning Property of Mortars with TiO_2 Addition Using Real Diesel Exhaust Soot. *J. Clean. Prod.* **2017**, *161*, 850–859. [CrossRef]

4. Dantas, S.R.A.; Vittorino, F.; Loh, K. Comparison of Reflectance to Solar Radiation between Mortars Treated with TiO2 and Painted Mortars after Three Years of Exposure. *J. Build. Eng.* **2022**, *46*, 103829. [CrossRef]
5. Schreck, M.; Niederberger, M. Photocatalytic Gas Phase Reactions. *Chem. Mater.* **2019**, *31*, 597–618. [CrossRef]
6. Sakar, M.; Mithun Prakash, R.; Trong-On, D. Insights into the Tio2-Based Photocatalytic Systems and Their Mechanisms. *Catalysts* **2019**, *9*, 680. [CrossRef]
7. Kumar, A.; Kumar, A.; Krishnan, V. Perovskite Oxide Based Materials for Energy and Environment-Oriented Photocatalysis. *ACS Catal.* **2020**, *10*, 10253–10315. [CrossRef]
8. Khan, S.; Park, J.S.; Ishihara, T. A Review of the Single-Step Flame Synthesis of Defective and Heterostructured TiO_2 Nanoparticles for Photocatalytic Applications. *Catalysts* **2023**, *13*, 196. [CrossRef]
9. Yang, L.; Hakki, A.; Zheng, L.; Jones, M.R.; Wang, F.; Macphee, D.E. Photocatalytic Concrete for NOx Abatement: Supported TiO2 Efficiencies and Impacts. *Cem. Concr. Res.* **2019**, *116*, 57–64. [CrossRef]
10. Constantino, J.C.P.; Garcia, D.C.S.; Palhares, H.G.; Houmard, M.; Figueiredo, R.B. Development of Functional TiO2 Coatings Deposited on Cementitious Materials. *Constr. Build. Mater.* **2020**, *250*, 118732. [CrossRef]
11. Poon, C.S.; Cheung, E. NO Removal Efficiency of Photocatalytic Paving Blocks Prepared with Recycled Materials. *Constr. Build. Mater.* **2007**, *21*, 1746–1753. [CrossRef]
12. Ibrahim, A.; Phoohinkong, W.; Mekprasart, W.; Pecharapa, W. Anatase/Rutile TiO2 Composite Thin Films Prepared via Dip Coating Technique and Their Hydrophilicity, Stability and Photocatalytic Activity. *Mater. Today Proc.* **2018**, *5*, 10903–10909. [CrossRef]
13. Croce, S.; D'Agnolo, E.; Caini, M.; Paparella, R. The Use of Cool Pavements for the Regeneration of Industrial Districts. *Sustain.* **2021**, *13*, 6322. [CrossRef]
14. Mansouri, O.; Belarbi, R.; Bourbia, F. Albedo Effect of External Surfaces on the Energy Loads and Thermal Comfort in Buildings. *Energy Procedia* **2017**, *139*, 571–577. [CrossRef]
15. Ramos, N.M.M.; Souza, A.R.; Maia, J.; Almeida, R.M.S.F. Colour Degradation of Façade Coatings - The Effect of Nanopigments Incorporation. *E3S Web Conf.* **2020**, *172*, 24004. [CrossRef]
16. Yuxuan, Z.; Yunyun, Z.; Jianrong, Y.; Xiaoqiang, Z. Energy Saving Performance of Thermochromic Coatings with Different Colors for Buildings. *Energy Build.* **2020**, *215*, 109920. [CrossRef]
17. Jimenez-Relinque, E.; Rodriguez-Garcia, J.R.; Castillo, A.; Castellote, M. Characteristics and Efficiency of Photocatalytic Cementitious Materials: Type of Binder, Roughness and Microstructure. *Cem. Concr. Res.* **2015**, *71*, 124–131. [CrossRef]
18. Cárdenas, C.; Tobón, J.I.; García, C.; Vila, J. Functionalized Building Materials: Photocatalytic Abatement of NO x by Cement Pastes Blended with TiO_2 Nanoparticles. *Constr. Build. Mater.* **2012**, *36*, 820–825. [CrossRef]
19. Mohseni, E.; Khotbehsara, M.M.; Naseri, F.; Monazami, M.; Sarker, P. Polypropylene Fiber Reinforced Cement Mortars Containing Rice Husk Ash and Nano-Alumina. *Constr. Build. Mater.* **2016**, *111*, 429–439. [CrossRef]
20. Diamanti, M.V.; Del Curto, B.; Ormellese, M.; Pedeferri, M.P. Photocatalytic and Self-Cleaning Activity of Colored Mortars Containing TiO_2. *Constr. Build. Mater.* **2013**, *46*, 167–174. [CrossRef]
21. Shen, W.; Zhang, C.; Li, Q.; Zhang, W.; Cao, L.; Ye, J. Preparation of Titanium Dioxide Nano Particle Modified Photocatalytic Self-Cleaning Concrete. *J. Clean. Prod.* **2015**, *87*, 762–765. [CrossRef]
22. Infibra. *Manual de Instalação—Placas Cimentícias NTF*; Infibra: Leme, Brazil, 2021.
23. Brasilit. *Catálogo de Produtos Brasilit: Soluções Para Telhados e Construções Industrializadas*; Brasilit: Brasilit, Brazil, 2018.
24. Valcan. *Ceramapanel Technical Information A1*; Valcan: Bridgwater, UK, 2022; pp. 3–4.
25. *NBR 7215*; Cimento Portland—Determinação Da Resistência à Compressão de Corpos de Prova Cilíndricos. ABNT: Rio de Janeiro, Brazil, 2019.
26. *NBR 13276*; Argamassa Para Assentamento e Revestimento de Paredes e Tetos—Determinação Do Índice de Consistência. ABNT: Rio de Janeiro, Brazil, 2016.
27. *NBR 13278*; Argamassa Para Assentamento e Revestimento de Paredes e Tetos—Determinação Da Densidade de Massa e Do Teor de Ar Incorporado. ABNT: Rio de Janeiro, Brazil, 2005.
28. *NBR 15498*; Placa de Fibrocimento Sem Amianto—Requisitos e Métodos de Ensaio. ABNT: Rio de Janeiro, Brazil, 2021.
29. *UNI 11259*; Photocatalysis—Determination of the Photocatalytic Activity of Hidraulic Binders—Rodammina Test Method. UNI: Milan, Italy, 2016.
30. *ASTM C1378-04(2014)*; Standard Test Method for Determination of Resistance to Staining. American National Standards Institute: West Conshohocken, PA, USA, 2014.
31. Rosales, A.; Maury-Ramírez, A.; De Gutiérrez, R.M.; Guzmán, C.; Esquivel, K. SiO2@TiO2 Coating: Synthesis, Physical Characterization and Photocatalytic Evaluation. *Coatings* **2018**, *8*, 120. [CrossRef]